Activity in the rat olfactory cortex is correlated with behavioral response to odor: a microPET study

Philippe Litaudon, Caroline Bouillot, Luc Zimmer, Nicolas Costes, Nadine Ravel

Activity in the rat olfactory cortex is correlated with behavioral response to odor: a microPET study

Philippe Litaudon[1], Caroline Bouillot[2], Luc Zimmer[1,2,3], Nicolas Costes[2], Nadine Ravel[1]

[1] Lyon Neuroscience Research Center, CNRS UMR 5292, INSERM U1028, Université Claude Bernard Lyon 1, CH Le Vinatier Bâtiment 452, 95 Bd Pinel, 69675 BRON Cedex, France

[2] CERMEP-Imagerie du Vivant, 59 Boulevard Pinel, 69677 Bron, France

[3] Hospices Civils de Lyon, Lyon, France

Corresponding author :

Philippe Litaudon

Lyon Neuroscience Research Center, Team « Olfaction : from coding to memory », 50 avenue Tony Garnier, 69366 LYON CEDEX, FRANCE

Email: philippe.litaudon@cnrs.fr

Phone number: +33 4 37 28 74 61

Fax number: +33 4 37 28 76 01

Acknowledgements

This work was supported by the LABEX CORTEX (ANR-11-LABX-0042) and the LABEX PRIMES (ANR-11-LABX-0063) of Université de Lyon, within the program "Investissements d'Avenir" (ANR-11-IDEX-0007) operated by the French National Research Agency (ANR).

Abstract

How olfactory cortical areas interpret odor maps evoked in the olfactory bulb and translate odor information into behavioral responses is still largely unknown. Indeed, rat olfactory cortices encompass an extensive network located in the ventral part of the brain, thus complicating the use of invasive functional methods. In vivo imaging techniques that were previously developed for brain activation studies in humans have been adapted for use in rodents and facilitate the non-invasive mapping of the whole brain. In this study, we report an initial series of experiments designed to demonstrate that microPET is a powerful tool to investigate the neural processes underlying odor-induced behavioral response in a large-scale olfactory neuronal network.

After the intravenous injection of [^{18}F]Fluorodeoxyglucose ([^{18}F]FDG), awake rats were placed in a ventilated Plexiglas cage for 50 minutes, where odorants were delivered every 3 min for a 10-s duration in a random order. Individual behavioral responses to odor were classified into categories ranging from 1 (head movements associated with a short sniffing period in response to a few stimulations) to 4 (a strong reaction, including rearing, exploring and sustained sniffing activity, to several stimulations). After [^{18}F]FDG uptake, rats were anesthetized to perform a PET scan. This experimental session was repeated two weeks later using the same animals without odor stimulation to assess the baseline level of activation in each individual. Two voxel-based statistical analyses (SPM 8) were performed: i) a two sample paired t-test analysis contrasting baseline versus odor scan and ii) a correlation analysis between voxel FDG activity and behavioral score.

As expected, the contrast analysis between baseline and odor session revealed activations in various olfactory cortical areas. Significant increases in glucose metabolism were also observed in other sensory cortical areas involved in whisker movement and in several modules of the cerebellum involved in motor and sensory function. Correlation analysis provided new insight into these results. [^{18}F]FDG uptake was correlated with behavioral response in a large part of the anterior piriform cortex and in some lobules of the cerebellum, in agreement with previous data showing that both piriform cortex and cerebellar activity in humans can be driven by sniffing activity, which was closely related to the high behavioral scores observed in our experiment. The present data demonstrate that microPET imaging offers an original perspective for rat behavioral neuroimaging.

Keywords: olfaction, piriform cortex, sniffing, microPET, [^{18}F]Fluorodeoxyglucose

Introduction

Understanding sensory information processing, which is crucial for building representations of the world, is a major challenge in neuroscience. Numerous studies of various sensory modalities have clearly established several common features of sensory representations. One of the most important is the cortical topographic coding of stimuli. In the rodent olfactory system, early 2-deoxyglucose (2-DG) experiments to the most recent optical imaging studies have consistently shown that odorant compounds generate specific patterns of activity across the glomerular layer of the olfactory bulb (OB), the first central relay of olfactory stimulus processing (Sharp et al. 1975; Jourdan et al. 1980; Takahashi et al. 2004; Johnson and Leon 2007; Martin et al. 2007; Esclassan et al. 2012). The OB projects to several higher olfactory cortical structures that are collectively known as the primary olfactory cortex, which includes the anterior olfactory nucleus, olfactory tubercle, piriform cortex, cortical amygdala and entorhinal cortex (Scalia and Winans 1975; Haberly and Price 1977; Haberly 2001; Miyamichi et al. 2011). However, how olfactory cortices interpret the odor maps generated in the OB and translate odor information into behavioral response remains largely unknown. In the piriform cortex (PC), the largest olfactory cortical area, odorants are represented by sparse, distributed, and spatially overlapping neural ensembles (Haberly 2001; Illig and Haberly 2003; Litaudon et al. 2003; Rennaker et al. 2007; Poo and Isaacson 2009), and the orderly topography of odorant representation observed in the OB is not maintained (Haberly 2001; Ghosh et al. 2011; Sosulski et al. 2011). Nevertheless, one recent study suggested that another type of spatial organization emerges in PC that is based more on where pyramidal cells send their output rather than the input that they receive from the OB (Chen et al. 2014). By contrast, mitral cell projections from a single glomerulus are spatially segregated in the cortical amygdala, thereby partially retaining the spatial organization observed in the OB (Sosulski et al. 2011). Thus, different olfactory cortical regions may differ in functional organization and the distinct features of olfactory information that they process in combination with other brain areas remain poorly documented.

To address this problem, it is necessary to correlate the activity of a large brain network with odor-induced behavioral changes. Several functional approaches have been used to study odor processing in the rodent brain. Immediate early gene mapping provides cellular-resolution data across the whole brain, but requires the animal to be sacrificed after the experiment, thereby precluding longitudinal studies. Optical recording offers good temporal and spatial

resolution over a large field of view, but the ventral location of the primary olfactory cortex necessitates invasive surgery (Litaudon and Cattarelli 1994; Litaudon et al. 1997a). Electrophysiological approaches yield data with millisecond temporal resolution but restrict the field of view. Thus, the assessment of brain activity in an extensive neuronal network requires the use of a large number of recording electrodes. In vivo imaging techniques such as functional magnetic resonance imaging (fMRI) and positron emission tomography (PET), which were previously developed for brain activation studies in humans, have been adapted for rodents. These translational methods overcome the aforementioned limitations, thus facilitating the repetitive and non-invasive mapping of the entire brain. Although promising results have been obtained in the OB (Yang et al. 1998; Xu et al. 2000; Kida et al. 2002; Xu et al. 2003; Martin et al. 2007), recording a BOLD signal in deep brain structures such as the olfactory cortex in small animals remains a challenge. Indeed, most studies have used a surface receiving coil located above the dorsal part of the skull to maximize the contrast-to-noise ratio. Unfortunately, the sensitivity of these coils is not uniform, and the signal-to-noise ratio drops dramatically with increasing distance from the coil, thereby compromising brain activation studies of ventral structures. Moreover, most fMRI studies require the animal to be anesthetized, thus precluding the assessment of behaviorally relevant brain activation.

In the present work, we propose the use of recent developments in high-resolution dedicated small animal positron emission tomography systems (microPET) (Lancelot and Zimmer 2010) to demonstrate that this technique provides a new and complementary approach to studying odor processing in the rodent brain. MicroPET offers poor spatial resolution compared to other brain imaging techniques, which makes it difficult to assess activity in small brain areas. Nevertheless, with respect to odor processing, the extent of rodent olfactory cortical regions as well as the large and homogenous field of view afforded by PET partially compensates for this limited spatial resolution. The key advantage of microPET compared to other imaging approaches is that the PET radiotracer - [^{18}F]Fluorodeoxyglucose ([^{18}F]FDG) - allows the whole-brain function to be examined without the effects of anesthesia. The animal is awake and freely moving during [^{18}F]FDG uptake, allowing the assessment of brain activation when the animal is engaged in a behavioral task (Sung et al. 2009; Jang et al. 2009).

This technique was recently used to investigate regions of the brain involved in sensory and learning processing (Soto-Montenegro et al. 2009; Ravasi et al. 2011; Luyten et al. 2012). To our knowledge, [^{18}F]FDG microPET has never been used to investigate the functional organization of the rodent olfactory system. The present work reports an initial series of

microPET experiments designed to investigate the brain areas involved in odor processing during a passive detection task and to demonstrate that microPET is a powerful tool for the study of neural processing in relation to the odor-induced behavioral response in a large-scale olfactory neuronal network.

Material and methods

Subjects

Male Wistar rats (Charles River, L'Arbresle, France, n=12) weighing 300-350 g were housed in standard rat cages in a climate-controlled vivarium with a 12-h light-dark cycle. Except on the day of experiment, all rats were given free access to food and water. All experiments were conducted in accordance with European guidelines for the care of laboratory animals (2010/63/EU) and were approved by the Lyon 1 University Ethics Committee (permission BH2012-48). The animals were acclimatized to the experimental setup each day for one week prior to beginning the experiments to minimize stress induced by exposure to a novel environment.

Study design

Twelve hours prior to the experiments, the rats were food-deprived but were allowed free access to water. This restriction was applied to selectively maximize and homogenize [^{18}F]FDG uptake at the brain level (Fueger et al. 2006). The animals were anesthetized with isoflurane (5% for induction and 2–2.5% for maintenance), and an intravenous catheter was placed in the tail vein. Immediately after bolus [^{18}F]FDG injection (11 to 18 MBq, 500 µl), the catheter was removed and isoflurane was discontinued. The rats were placed in a dark ventilated Plexiglas cage, where they recovered from anesthesia for one or two minutes. We chose to use four different odorants to maintain the level of arousal achieved by odorant stimulation across the entire session and to avoid habituation due to repeated stimulation with the same odor. The four odorants, i.e., isoamyl acetate, 2-heptanone, eugenol, and (-)carvone (Sigma Aldrich, Saint-Quentin Fallavier, France), have been used in previous behavioral experiments and are easily discriminated (Chapuis et al. 2009; Courtiol et al. 2011; Courtiol et al. 2014; Torquet et al. 2014; Veyrac et al. 2015). The odors were delivered in a random order from the top of the cage using a custom-built flow dilution olfactometer at a concentration of

10^{-1} saturated vapor and a constant rate of 1.8 liter/min. The stimulations lasted ten seconds and were separated by a three-minute delay to limit odor adaptation. The [^{18}F]FDG uptake session lasted 50 min, corresponding to 17 olfactory stimulations. During [^{18}F]FDG uptake, animal behavior was monitored and recorded using an infra-red video camera. The behavioral response to each odor was analyzed off-line. At 50 min [^{18}F]FDG post-injection, the rats were anesthetized with isoflurane and subjected to a 20-minute PET scan.

The experiment was repeated two weeks later (sessions 1 & 2). Six rats were stimulated for 50 min during session #1 and were assessed without stimulation during session #2, whereas another set of six rats was tested without any stimulation during session #1 and with odor stimulation during session #2. This experimental design was chosen to include a control session, which is necessary to assess the baseline level of activation and to avoid any order effect of odor stimulation. We performed a total of 11 baseline scans (one rat died during FDG uptake) and 12 odor stimulation scans.

PET scanning

Data were acquired in list-mode using a dedicated small animal PET/CT scanner manufactured by Inveon (Siemens, Erlangen, Germany). The scanner has an axial field of view of 12.7 cm and a spatial resolution of 1.8 mm full width at half maximum (FWHM) (Bao et al. 2009). This nominal resolution means that two sources of the same activity separated by less than 1.8 mm cannot be distinguished. Nevertheless, smaller sources can be detected and quantified. Immediately following isoflurane anesthesia, the rats were placed in a prone position on the bed of the scanner, and an emission scan lasting 20 minutes was initiated. To minimize head movement, the rat was fixed with ear bars and a tooth bar in a head holder. Its body temperature was maintained at 37 ± 0.2 °C by means of a temperature-controlled circuit integrated into the dedicated bed. A CT scan was performed in the same position immediately after PET emission scan to correct for tissue attenuation. The images were reconstructed in four frames of five minutes each with attenuation as well as scatter correction by a 3D-filtered back-projection algorithm (Hamming filter; cut-off frequency 0.5 cycles/pixel) and a zoom factor of two. This led to reconstructed volumes of 159 slices comprising 128 × 128 voxels in a bounding box of 49.7 × 49.7 × 126 mm with voxel size 0.388 × 0.388 × 0.796 mm. After scanning, the animals were returned to their home cages.

Behavioral analysis

For each rat, an individual behavioral score was assessed according to the number and strength of the behavioral response to odor across a total of 17 stimulations. Exploratory behavior in response to odor varied from a simple head orientation associated with a short period of sniffing to rearing toward an odor source associated with a sustained sniffing activity. This resulted in the classification of each rat with a behavioral score ranging from 1 (less responsive) to 4 (highly responsive).

Data analyses

Data processing was carried out using statistical parametric mapping software (SPM8, Welcome trust center for neuroimaging, London; http://www.fil.ion.ucl.ac.uk/spm/). Individual PET images were spatially normalized to a custom PET [^{18}F]FDG template made from the MRI template in the space of the Lancelot rat brain atlas (Lancelot et al. 2014). Lancelot et al. (2014) showed that the sensitivity of detection in the subject space does not differ after spatially normalizing PET images in the template space *via* a functional template. Furthermore, this method resulted in excellent reproducibility. Two voxel-based statistical analyses were performed using SPM: a two-sample paired t-test analysis contrasting [^{18}F]FDG activity at baseline with odor condition, and a correlation analysis between voxel [^{18}F]FDG activity and behavioral score (determined on a scale of 0 to 4), with the score converted into a covariate. In the SPM analyses, voxel [^{18}F]FDG activities were normalized by proportional scaling using the whole-brain mean [^{18}F]FDG activity computed for each scan within the template mask of the brain. Clusters of significant detections were defined as follows: statistical maps were thresholded at $p<0.05$ (uncorrected), but only clusters of voxels exceeding 50 voxels (0.125 mm^3) and spaced by more than 1.8 mm were retained as significant. T-value maps of significant clusters were overlaid onto the MRI template, and the Lancelot atlas was used to identify brain structures.

Results

Behavioral data

Overall, the rats exhibited clear exploratory behavior in response to an odorant for 49% of the stimuli. This exploratory behavior varied from a simple head orientation associated with a short period of sniffing to a complete rearing toward the odor source associated with active sniffing activity. Each rat exhibited between 4 and 11 detectable behavioral responses among the 17 odor stimulations. The percentage of behavioral response was the same for all odors (Chi-square test, $p=0.99$), indicating that the level of behavioral modulation was not

dependent on odor identity. The number of behavioral responses was not significantly different according to the order of the measurement events (i.e., odor first or baseline first; Chi-square test, p=0.88). Finally, we tested how the behavioral response evolved across the [^{18}F]FDG uptake session by dividing the session into four periods. Even if a slight decrease in the prevalence of behavioral response was observed during the last period, there was no significant difference in the number of behavioral responses among the four periods (Chi-square test, p=0.11). Thus, the probability of observing a behavioral response did not significantly differ throughout the [^{18}F]FDG uptake session, indicating that the habituation to odor stimulation was limited. Thus, the behavioral profiles of the rats were classified into 4 categories, which ranged from 1 (head movements associated with short sniffing period in response to a few stimulations) to 4 (a strong reaction to several stimulations, including rearing, exploring and sustained sniffing activity): #1 (less responsive, n=2); #2 (weakly to moderately responsive, n=4); #3 (moderately to highly responsive, n=2); and #4 (highly responsive, n=3). During baseline measurements, the rats remained still in the cage throughout the [^{18}F]FDG uptake period, and a behavioral score of 0 was assigned. For the duration of the procedure, we did not observe any sign of pain or irritation in response to the odors (i.e., freezing, snout rubbing) that could be attributed to a trigeminal response. This is in agreement with previous data showing that rats exhibited neither spontaneous aversion nor preference for the odorants used in our experiments (Chapuis et al. 2009; Torquet et al. 2014).

PET data

An analysis based on image contrast between odor and baseline conditions was used to determine the brain regions activated by odor stimulus as well as those involved in a behavioral response induced by odor. This analysis revealed significant regional brain activations in several olfactory cortical areas (Table 1). A small cluster of significant voxels was observed in the anterior PC (aPC) (0.282 mm^3, Fig. 1a,b). Significant [^{18}F]FDG uptake was also observed in other olfactory cortical areas such as the entorhinal cortex and the cortical amygdala (Fig. 1e-g). No significant [^{18}F]FDG uptake was observed in other olfactory cortical areas, including the posterior PC, anterior olfactory nucleus, and olfactory tubercle. In addition to the olfactory system, significant increases in glucose metabolism were observed in other sensory cortical areas: the primary somatosensory cortex at the level of the barrel field of the primary somatosensory cortex (S1BF), the orofacial region, and the secondary somatosensory cortex (Fig. 1c-g). Finally, the contrast between odor and baseline sessions revealed activations in several modules of the cerebellum (Fig. 1h-j). We did not observe any

deactivation in response to odor stimulation. We also considered the possibility of an effect of the order of measurements (i.e., odor first or baseline first), but no significant differences were found for any brain region.

We next used a correlation analysis between voxel [^{18}F]FDG activity and behavioral score to assess whether the level of brain activity was correlated with the level of behavioral response induced by odorant stimulation (Table 2). In a large part of the aPC, [^{18}F]FDG uptake was correlated with behavioral response (Fig. 2a-c). This correlation was also observed in the cortical amygdala (Fig. 2e-g). As shown via contrast analysis, these olfactory cortical activations were lateralized and restricted to the left hemisphere. By contrast, there were no significant clusters in the barrel, visual and entorhinal cortices, indicating that the [^{18}F]FDG uptake increase revealed by the previous contrast analysis was not significantly correlated with rat behavioral response. Finally, the significant correlations between glucose metabolism and behavioral response in the cerebellum (Fig. 2h-j) were restricted to three modules (Crus 2, PM, COP).

Discussion

The present study is the first to demonstrate that [18F]FDG microPET is a powerful tool to study odor representation in large-scale rodent neuronal networks. Our first analysis, based on the image contrast between odor and baseline conditions, revealed limited activation in several cortical olfactory structures. Indeed, only a small cluster of significant voxels was reported in the aPC. This result is in agreement with data showing that odors evoked sparse activation in the aPC, where only 10 to 20% of neurons responded to odors (Litaudon et al. 2003; Rennaker et al. 2007; Poo and Isaacson 2009; Zhan and Luo 2010). Such relatively low activity might not be detected due to the lower sensitivity of PET imaging compared to electrophysiological recording. The paradigm that we used did not require any behavioral action or timing, and the absence of such events could also explain this result. Indeed, previous data (Schoenbaum and Eichenbaum 1995; Zinyuk et al. 2001) reported that when the animals were engaged in a discrimination task, a large proportion of piriform neurons were more significantly involved in task event-related activity (e.g., nose poking and water delivery) than in pure odor coding. Significant [18F]FDG uptake was also observed in the entorhinal cortex and cortical amygdala, which receive direct projections from the OB and have been reported to respond to odors (Scalia and Winans 1975; Haberly and Price 1977; Haberly 2001; Miyamichi et al. 2011; Xu and Wilson 2012; Chapuis et al. 2013). The activation observed in the cortical amygdala might also be explained by an odor-induced

emotional reaction. Although we did not observe freezing behavior in response to odor, the first odor stimulations were delivered immediately after anesthesia recovery and could have been associated with malaise induced by isoflurane inhalation. Odor vs baseline contrast analysis did not reveal activation in the anterior olfactory nucleus or in the olfactory tubercle. Although odor responses have been reported in these structures in anesthetized animals, few studies have been conducted in awake rodents, thus making it difficult to interpret our results. Apart from the issue of microPET sensitivity, it should be noted that recent studies in awake mice have shown that olfactory tubercle neurons encode either odor valence (Gadziola et al. 2015) or the biological significance of the odor (Rampin et al. 2012). However, the odors used in our experiment possess neither inherent biological significance nor acquired valence.
Apart from the olfactory system, odor stimulation evoked increases in glucose metabolism in somatosensory cortical areas. These activations could be explained by whisker movements, which are coupled with sniffing during environmental exploration (Welker 1964; Deschênes et al. 2012). Finally, the extensive activations observed in the cerebellum are consistent with its role in motor and sensory function. Indeed, the rats remained motionless in the experimental cage during most baseline measurements, whereas odor delivery evoked a motor response; this likely explains the increase in [^{18}F]FDG uptake observed in this cerebral structure. Overall, our contrast analysis was in agreement with the sensory and motor responses induced by odor stimulation.

Correlation analysis provides new insight into our results. For this analysis, the behavioral score was added as a covariate. Interestingly, this analysis revealed a high correlation between glucose metabolism in the aPC and behavioral response. This correlation might be explained by the obvious change in sniffing behavior reported for rats exhibiting high behavioral response scores and is in agreement with previous data showing that PC activity could be driven by sniffing alone, both in human (Sobel et al. 1998a; Sobel et al. 2000) and rat (Fontanini et al. 2003). Such sniffing-related activity could be explained by the mechanical sensitivity of olfactory sensory neurons (Grosmaitre et al. 2007), which could drive airflow-related activity in the OB (Courtiol et al. 2011). As afferent connections from the OB are predominant in the aPC (Haberly 1973; Schwob and Price 1978), a tight functional coupling between OB and aPC (Chabaud et al. 1999; Litaudon et al. 2003; Litaudon et al. 2008) could explain this pronounced sniffing-related activity. In other olfactory cortical areas, cellular activity appeared to be less entrained by respiration. This has been reported both in the

olfactory tubercle (Rampin et al. 2012) and in the lateral entorhinal cortex (Xu and Wilson 2012).

The use of only four different odors during the odor session does not allow us to rule out the hypothesis of topographic "coding" of odor quality in the piriform cortex. Nevertheless, the large extent of aPC activation agrees with the absence of an orderly topography of odorant representation in this cortex (Haberly 2001; Sosulski et al. 2011; Gire et al. 2013). It must be noted that we did not observe any significant activation in the posterior PC, which has been reported to be more involved in associative memory processes that are not required in this experiment (Litaudon et al. 1997b).

The results obtained at the cerebellum level converge with previous data showing that the Crus 2 and PM lobules are activated by whisker stimulation (Sharp and Gonzalez 1985; Bosman et al. 2010) and by stimulation of the skin of the snout (Armstrong and Drew 1980). Significant responses to odor were associated with elevation movements toward the odor source, which explains the activation of the COP. Indeed, this cerebellar module exhibited an increase in 2-DG uptake when electrical stimulations were delivered to the hindlimb motor/sensory cortex (Sharp et al. 1989). Finally, this result is consistent with an fMRI study performed in human showing that the cerebellum was also activated by the sniffing response (Sobel et al. 1998b). Indeed, in our experiment, clear change in sniffing behavior was closely related with high behavioral scores.

One unexpected result was the lateralization of activation of the olfactory cortices, even though the odorant stimulation was not lateralized. What is the origin of this asymmetry? In rat, there is variation in the airflow rate between the two nostrils during a nasal cycle of 30-85 minutes (Bojsen-Moller and Fahrenkrug 1971). Nevertheless, to account for the lateralization observed in the present study, these changes in nasal airflow must be synchronized between animals. It is more probable that this asymmetry reflects functional differences between hemispheres. Brain function lateralization has been extensively described in human brain regions, including olfactory structures (Royet and Plailly 2004). Moreover, several studies have demonstrated that lateralization of cortical functions is not an exclusive feature of the human brain, and hemispheric dominance and lateralization of cortical functions have been reported for a great variety of animal species (Corballis 2008). Indeed, lateralization of vestibular information processing has been reported previously using FDG microTEP in rats with a predominance of left hemisphere (Best et al. 2014). Interestingly, the lateralization of odor processing was recently shown in the rat piriform cortex during an olfactory

discrimination learning task (Cohen et al. 2015), with a predominance of the left hemisphere similar to that reported in our data.

Several technical issues must be considered when using FDG microPET. First, the temporal resolution of this technique is poor compared to that of other functional methods. Indeed, [^{18}F]FDG is irreversibly trapped within tissues over the course of the uptake session, and the final PET image is the cumulative result of all brain activations occurring during FDG uptake. Thus, it is not possible with our experimental design to estimate the changes in brain metabolism evoked by a single odorant molecule. Second, the spatial resolution of this technique is limited, making it difficult to assess the activity of small brain areas, or, for example, to analyze odor-specific patterns of activity in the olfactory bulb at the glomerular level, as can be achieved with fMRI (Martin et al. 2007) and optical recording (Esclassan et al. 2012). However, both fMRI and optical imaging studies require the animal to be anesthetized or head-fixed, thus precluding an assessment of behavior-related brain activation. During microPET, probe uptake occurs while the animal is conscious and freely moving. Thus, this technique allows the examination of whole brain function without the confounding effects of anesthesia or animal sacrifice, and enables studies that require serial brain imaging of the same subject. Moreover, as demonstrated by our study, it is possible using this technique to assess the relationship between brain activation and animal behavior. If the use of [^{18}F]FDG requires its accumulation over the course of tens of minutes, microPET imaging is appropriate for use in conjunction with several behavioral paradigms (e.g., odor discrimination in a go-no go task) that require task repetition by the animal. MicroPET should also be considered as a complementary approach to electrophysiological recording. By assessing whole brain activity, even at low spatial resolution, this technique could help to define areas of interest for subsequent electrophysiological recording, thereby reducing the number of implanted electrodes necessary to acquire meaningful data. Overall, our results demonstrate that microPET imaging offers an original perspective for rat behavioral neuroimaging.

Ethical approval: All applicable international, national, and/or institutional guidelines for the care and use of animals were followed. All procedures received approval from the Lyon 1 University Ethics Committee (permission BH2012-48).

Informed consent: This article does not contain any studies with human participants performed by any of the authors.

Conflict of Interest: The authors declare that they have no conflict of interest.

References

Armstrong DM, Drew T (1980) Responses in the posterior lobe of the rat cerebellum to electrical stimulation of cutaneous afferents to the snout. J Physiol 309:357–374.

Best C, Lange E, Buchholz H-G, et al (2014) Left hemispheric dominance of vestibular processing indicates lateralization of cortical functions in rats. Brain Struct Funct 219:2141–2158. doi: 10.1007/s00429-013-0628-1

Bojsen-Moller F, Fahrenkrug J (1971) Nasal swell-bodies and cyclic changes in the air passage of the rat and rabbit nose. J Anat 110:25–37.

Bosman LWJ, Koekkoek SKE, Shapiro J, et al (2010) Encoding of whisker input by cerebellar Purkinje cells. J Physiol 588:3757–3783. doi: 10.1113/jphysiol.2010.195180

Chabaud P, Ravel N, Wilson DA, Gervais R (1999) Functional coupling in rat central olfactory pathways: a coherence analysis. Neurosci Lett 276:17–20.

Chapuis J, Cohen Y, He X, et al (2013) Lateral entorhinal modulation of piriform cortical activity and fine odor discrimination. J Neurosci 33:13449–13459. doi: 10.1523/JNEUROSCI.1387-13.2013

Chapuis J, Garcia S, Messaoudi B, et al (2009) The way an odor is experienced during aversive conditioning determines the extent of the network recruited during retrieval: a multisite electrophysiological study in rats. J Neurosci 29:10287–98. doi: 10.1523/JNEUROSCI.0505-09.2009

Chen C-FF, Zou D-J, Altomare CG, et al (2014) Nonsensory target-dependent organization of piriform cortex. Proc Natl Acad Sci U S A 111:16931–16936. doi: 10.1073/pnas.1411266111

Cohen Y, Putrino D, Wilson DA (2015) Dynamic cortical lateralization during olfactory discrimination learning. J Physiol 593:1701–1714. doi: 10.1113/jphysiol.2014.288381

Corballis MC (2008) Of mice and men - and lopsided birds. Cortex 44:3–7. doi: 10.1016/j.cortex.2007.10.001

Courtiol E, Amat C, Thevenet M, et al (2011) Reshaping of bulbar odor response by nasal flow rate in the rat. PLoS One 6:e16445. doi: 10.1371/journal.pone.0016445

Courtiol E, Lefèvre L, Garcia S, et al (2014) Sniff adjustment in an odor discrimination task in the rat: analytical or synthetic strategy? Front Behav Neurosci 8:145. doi: 10.3389/fnbeh.2014.00145

Deschênes M, Moore J, Kleinfeld D (2012) Sniffing and whisking in rodents. Curr Opin Neurobiol 22:243–250. doi: 10.1016/j.conb.2011.11.013

Esclassan F, Courtiol E, Thevenet M, et al (2012) Faster, deeper, better: the impact of sniffing modulation on bulbar olfactory processing. PLoS One 7:e40927. doi: 10.1371/journal.pone.0040927

Fontanini A, Spano P, Bower JM (2003) Ketamine-xylazine-induced slow (<1.5 Hz) oscillations in the rat piriform (olfactory) cortex are functionally correlated with respiration. J Neurosci 23:7993–8001.

Fueger BJ, Czernin J, Hildebrandt I, et al (2006) Impact of animal handling on the results of 18F-FDG PET studies in mice. J Nucl Med 47:999–1006.

Gadziola MA, Tylicki KA, Christian DL, Wesson DW (2015) The olfactory tubercle encodes odor valence in behaving mice. J Neurosci 35:4515–4527. doi: 10.1523/JNEUROSCI.4750-14.2015

Ghosh S, Larson SD, Hefzi H, et al (2011) Sensory maps in the olfactory cortex defined by long-range viral tracing of single neurons. Nature 472:217–220. doi: 10.1038/nature09945

Gire DH, Whitesell JD, Doucette W, Restrepo D (2013) Information for decision-making and stimulus identification is multiplexed in sensory cortex. Nat Neurosci 16:991–993. doi: 10.1038/nn.3432

Grosmaitre X, Santarelli LC, Tan J, et al (2007) Dual functions of mammalian olfactory sensory neurons as odor detectors and mechanical sensors. Nat Neurosci 10:348–54. doi: 10.1038/nn1856

Haberly LB (2001) Parrallel-distributed processing in olfactory cortex: new insights from morphological and physiological analysis of neuronal circuitry. Chem Senses 26:551–576. doi: 10.1093/chemse/26.5.551

Haberly LB (1973) Summed potentials evoked in opossum prepyriform cortex. J Neurophysiol 36:775–788.

Haberly LB, Price JL (1977) The axonal projection patterns of the mitral and tufted cells of the olfactory bulb in the rat. Brain Res 129:152–157.

Illig KR, Haberly LB (2003) Odor-evoked activity is spatially distributed in piriform cortex. J Comp Neurol 457:361–373. doi: 10.1002/cne.10557

Jang D-P, Lee S-H, Lee S-Y, et al (2009) Neural responses of rats in the forced swimming test: [F-18]FDG micro PET study. Behav Brain Res 203:43–47. doi: 10.1016/j.bbr.2009.04.020

Johnson BA, Leon M (2007) Chemotopic odorant coding in a mammalian olfactory system. J Comp Neurol 503:1–34. doi: 10.1002/cne.21396

Jourdan F, Duveau A, Astic L, Holley A (1980) Spatial distribution of [14C]-2-deoxyglucose uptake in the olfactory bulbs of rats stimulated with two different odours. Brain Res 188:139–154.

Kida I, Xu F, Shulman RG, Hyder F (2002) Mapping at glomerular resolution: fMRI of rat olfactory bulb. Magn Reson Med 48:570–576. doi: 10.1002/mrm.10248

Lancelot S, Roche R, Slimen A, et al (2014) A multi-atlas based method for automated anatomical rat brain MRI segmentation and extraction of PET activity. PloS One 9:e109113. doi: 10.1371/journal.pone.0109113

Lancelot S, Zimmer L (2010) Small-animal positron emission tomography as a tool for neuropharmacology. Trends Pharmacol Sci 31:411–417. doi: 10.1016/j.tips.2010.06.002

Litaudon P, Amat C, Bertrand B, et al (2003) Piriform cortex functional heterogeneity revealed by cellular responses to odours. Eur J Neurosci 17:2457–2461. doi: 10.1046/j.1460-9568.2003.02654.x

Litaudon P, Cattarelli M (1994) Multisite recordings of the brain in the in vivo rat using a voltage-sensitive dye. Neurosci Prot 070-02: 1-15.

Litaudon P, Datiche F, Cattarelli M (1997a) Optical recording of the rat piriform cortex activity. Prog Neurobiol 52:485–510.

Litaudon P, Garcia S, Buonviso N (2008) Strong coupling between pyramidal cell activity and network oscillations in the olfactory cortex. Neuroscience 156:781–787.

Litaudon P, Mouly A-M, Sullivan R, et al (1997b) Learning-induced changes in rat piriform cortex mapped using multisite recording with voltage-sensitive dye. Eur J Neurosci 8:1593–1602.

Luyten L, Casteels C, Vansteenwegen D, et al (2012) Micro-positron emission tomography imaging of rat brain metabolism during expression of contextual conditioning. J Neurosci 32:254–263. doi: 10.1523/JNEUROSCI.3701-11.2012

Martin C, Grenier D, Thévenet M, et al (2007) fMRI visualization of transient activations in the rat olfactory bulb using short odor stimulations. Neuroimage 36:1288–1293. doi: 10.1016/j.neuroimage.2007.04.029

Miyamichi K, Amat F, Moussavi F, et al (2011) Cortical representations of olfactory input by trans-synaptic tracing. Nature 472:191–196. doi: 10.1038/nature09714

Paxinos G, Watson C (2005) The rat brain in stereotaxic coordinates. Elsevier Academic Press, Sidney.

Poo C, Isaacson JS (2009) Odor representations in olfactory cortex: “sparse” coding, global inhibition, and oscillations. Neuron 62:850–861. doi: 10.1016/j.neuron.2009.05.022

Rampin O, Bellier C, Maurin Y (2012) Electrophysiological responses of rat olfactory tubercle neurons to biologically relevant odours. Eur J Neurosci 35:97–105. doi: 10.1111/j.1460-9568.2011.07940.x

Ravasi L, Shimoji K, Soto-Montenegro ML, et al (2011) Use of [18F]fluorodeoxyglucose and the ATLAS small animal PET scanner to examine cerebral functional activation by whisker stimulation in unanesthetized rats. Nucl Med Commun 32:336–342. doi: 10.1097/MNM.0b013e3283447292

Rennaker RL, Chen CF, Ruyle AM, et al (2007) Spatial and temporal distribution of odorant-evoked activity in the piriform cortex. J Neurosci 27:1534–1542. doi: 10.1523/JNEUROSCI.4072-06.2007

Royet J-P, Plailly J (2004) Lateralization of olfactory processes. Chem Senses 29:731–745. doi: 10.1093/chemse/bjh067

Scalia F, Winans SS (1975) The differential projections of the olfactory bulb and accessory olfactory bulb in mammals. J Comp Neurol 161:31–55. doi: 10.1002/cne.901610105

Schoenbaum G, Eichenbaum H (1995) Information coding in the rodent prefrontal cortex.1. Single-neuron activity in orbitofrontal cortex compared with that in pyriform cortex. J Neurophysiol 74:733–750.

Schwob JE, Price JL (1978) The cortical projections of the olfactory bulb: development in fetal and neonatal rats with additional observations in the adult. Brain Res 151:369–374.

Sharp FR, Gonzalez MF (1985) Multiple vibrissae sensory regions in rat cerebellum: a (14C) 2-deoxyglucose study. J Comp Neurol 234:489–500. doi: 10.1002/cne.902340407

Sharp FR, Gonzalez MF, Sharp JW, Sagar SM (1989) c-fos expression and (14C) 2-deoxyglucose uptake in the caudal cerebellum of the rat during motor/sensory cortex stimulation. J Comp Neurol 284:621–636. doi: 10.1002/cne.902840409

Sharp FR, Kauer JS, Shepherd GM (1975) Local sites of activity-related glucose metabolism in rat olfactory bulb during olfactory stimulation. Brain Res 98:596–600.

Sobel N, Prabhakaran V, Desmond JE, et al (1998a) Sniffing and smelling: separate subsystems in the human olfactory cortex. Nature 392:282–286. doi: 10.1038/32654

Sobel N, Prabhakaran V, Hartley CA, et al (1998b) Odorant-induced and sniff-induced activation in the cerebellum of the human. J Neurosci 18:8990–9001.

Sobel N, Prabhakaran V, Zhao Z, et al (2000) Time course of odorant-induced activation in the human primary olfactory cortex. J Neurophysiol 83:537–551.

Sosulski DL, Bloom ML, Cutforth T, et al (2011) Distinct representations of olfactory information in different cortical centres. Nature 472:213–216. doi: 10.1038/nature09868

Soto-Montenegro ML, Vaquero JJ, Pascau J, et al (2009) Detection of visual activation in the rat brain using 2-deoxy-2-[(18)F]fluoro-D: -glucose and statistical parametric mapping (SPM). Mol Imaging Biol 11:94–99. doi: 10.1007/s11307-008-0179-7

Sung K-K, Jang D-P, Lee S, et al (2009) Neural responses in rat brain during acute immobilization stress: a [F-18]FDG micro PET imaging study. NeuroImage 44:1074–1080. doi: 10.1016/j.neuroimage.2008.09.032

Takahashi YK, Kurosaki M, Hirono S, Mori K (2004) Topographic representation of odorant molecular features in the rat olfactory bulb. J Neurophysiol 92:2413–2427. doi: 10.1152/jn.00236.2004

Torquet N, Aimé P, Messaoudi B, et al (2014) Olfactory preference conditioning changes the reward value of reinforced and non-reinforced odors. Front Behav Neurosci 8:229. doi: 10.3389/fnbeh.2014.00229

Veyrac A, Allerborn M, Gros A, et al (2015) Memory of occasional events in rats: individual episodic memory profiles, flexibility, and neural substrate. J Neurosci 35:7575–7586. doi: 10.1523/JNEUROSCI.3941-14.2015

Welker WI (1964) Analysis of sniffing of the albino rat. Behavior 22:223–244.

Xu F, Kida I, Hyder F, Shulman RG (2000) Assessment and discrimination of odor stimuli in rat olfactory bulb by dynamic functional MRI. Proc Nat Acad Sci USA 19:10601–10606. doi: 10.1073/pnas.180321397

Xu F, Liu N, Kida I, et al (2003) Odor maps of aldehydes and esters revealed by functional MRI in the glomerular layer of the mouse olfactory bulb. Proc Natl Acad Sci USA 100:11029–11034. doi: 10.1073/pnas.1832864100

Xu W, Wilson DA (2012) Odor-evoked activity in the mouse lateral entorhinal cortex. Neuroscience 223:12–20. doi: 10.1016/j.neuroscience.2012.07.067

Yang X, Renken R, Hyder F, et al (1998) Dynamic mapping at the laminar level of odor-elicited responses in rat olfactory bulb by functional MRI. Proc Nat Acad Sci USA 95:7715–7720.

Zhan C, Luo M (2010) Diverse patterns of odor representation by neurons in the anterior piriform cortex of awake mice. J Neurosci 30:16662–72. doi: 10.1523/JNEUROSCI.4400-10.2010

Zinyuk LE, Datiche F, Cattarelli M (2001) Cell activity in the anterior piriform cortex during an olfactory learning in the rat. Behav Brain Res 124:29–32.

Figure legends

Fig. 1 Voxel-based SPM results for the T-contrast odor versus baseline.

From a to j: Coronal slices through T-maps showing clusters of significant increases in [^{18}F]FDG uptake overlaid on an MRI template. The images follow radiological convention.

Fig. 2

Coronal MRI brain sections with overlays indicating the regions where statistically significant correlations between [^{18}F]FDG uptake and behavioral score were observed. The images follow radiological convention.

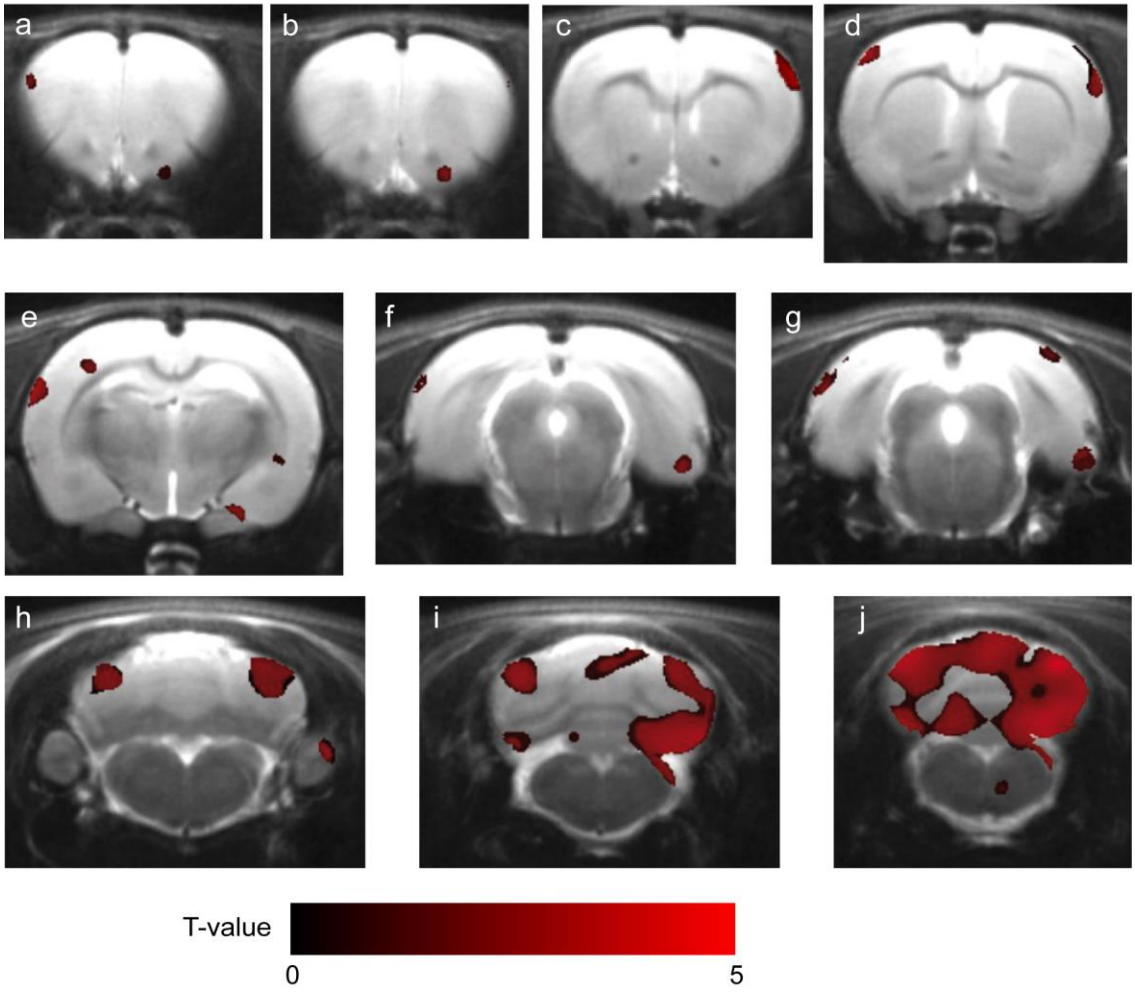

Figure 1

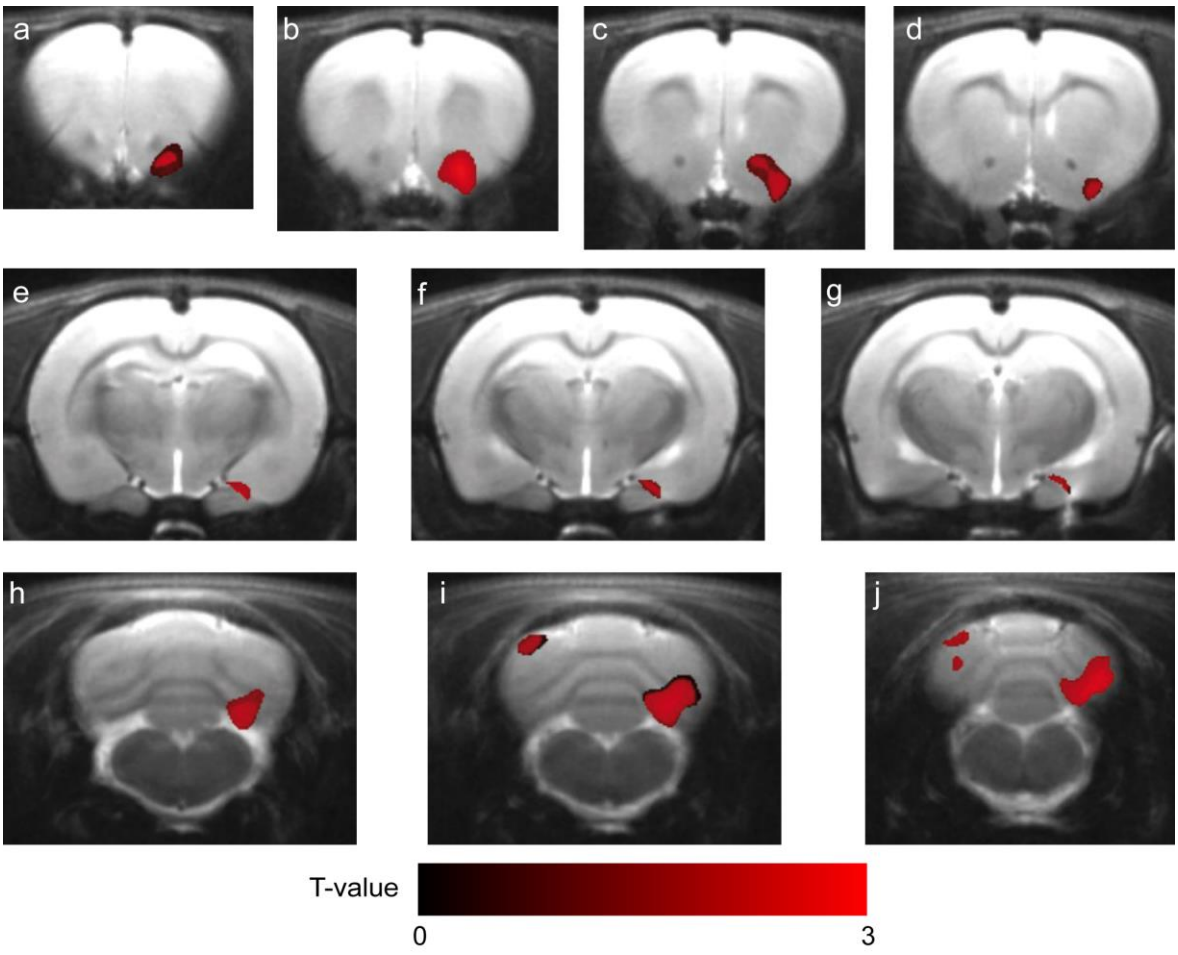

Figure 2

Table 1: Brain regions showing glucose metabolism increase during odor condition compared to baseline.

Brain area	Fig. 1 panel	Cluster size (mm^3)	Cluster Peak		Coordinates (mm)		
			T-value	p-value	x	y	z
M1	a	0,102	1.94	0.039	4.6	-3.5	3.5
aPC	a, b	0,282	1.98	0.037	-2.1	-8.0	3.0
S1 (right)	d	1,674	3.20	0.005	-5.9	-3.3	1.2
S1 (left)	c,d	0,738	2.80	0.009	5.5	-2.5	0.2
Barrel cortex	e	2,072	3.36	0.004	7.0	-4.0	-2.3
Cortical amygdala	e	0,418	2.24	0.024	-3.1	-10.2	-2.5
Entorhinal cortex	f-g	0,656	2.25	0.024	-6.8	-7.0	-8.5
Visual cortex	g	1,160	2.43	0.018	-4.9	-2.2	-9.0
Cerebellum	h-j	59,048	4.26	0.001	-3.7	-3.9	-14.0

Values x, y, z are the coordinates of the peak activation centers in the Paxinos and Watson stereotaxic space (Paxinos and Watson, 2005). The x-coordinate corresponds to the distance lateral from the midline between the hemispheres (positive values for spots located on the right side); the y-coordinate denotes the dorsoventral position; the z-coordinate indicates the position relative to Bregma (positive values for sections anterior to Bregma).

Table 2: Brain regions showing significant correlation between [^{18}F]FDG uptake and behavioral score.

Brain area	Fig. 2 panel	Cluster size (mm^3)	Cluster Peak		Coordinates (mm)		
			T-value	p-value	x	y	z
aPC	a-d	3,826	2.74	0.006	-2.1	-8.0	3.0
Cortical amygdala	e-g	0,658	2.17	0.021	-2.9	-10.1	-2.5
Cerebellum (Crus 2)	i-j	1,100	1.92	0.034	3,3	-3.1	-13.8
Cerebellum (COP/PM)	h-j	4,706	2.36	0.014	-3.8	-5.8	-14.0

Values x, y, z are the Paxinos and Watson coordinates (x: left to right, y: ventral to dorsal, z: posterior to anterior, see Table 1).